2014 International Conference on Unmanned Aircraft Systems (ICUAS)
May 27-30, 2014. Orlando, FL, USA

Development of Control System for an Unmanned Single Tilt Tri-Rotor Aerial Vehicle

Andrzej Ryś, Roman Czyba and Grzegorz Szafrański

Abstract— **This paper outlines the mechanical design, hardware, measurement system and control system architecture with particular emphasis on the practical aspects of the control implementation for an unmanned aerial vehicle type trirotor. The main investigated area is the attitude control system. Various practical implementations of PID controller were studied, including algorithms with modified loop structures and cascade systems. Furthermore, an embedded microcontroller-based navigation and control system is proposed to provide efficient angular stabilization and stable hover during the different flight conditions. The design, analysis and the validation tests have been undertaken on the experimental aerial platform.**

I. INTRODUCTION

Unmanned Aerial Vehicles (UAVs) were first introduced in battlefields of World War I in 1917. Mainly due to existing technical limitations at this time, the first UAVs were large, slow and unreliable. As such, they could not play any important role and affect battles results. The most important event in the history of development of UAVs, was the terrorist attack on 9/11 followed by the war in Afghanistan and Operation Iraqi Freedom. From this time, UAVs can be found on front covers, news and TV documentaries. Number of successful missions employing UAVs resulted in enormous growth of military and commercial UAVs market. The market research by Teal Group 2013 predicts that UAVs expenditures will more than double over the next decade, from current worldwide UAVs spending of $5.2 billion annually to $11.6 billion, totaling just over $89 billion in the next ten years. This makes the UAV sector the most dynamic growth sector of the world aerospace industry [16].

It is crucial to state that unmanned air vehicles are mostly used for military applications, however vertical take-off and landing (VTOL) vehicles applications are moving to the non-military domains as well. UAVs applications include exploration, inspection and surveillance of sites that are hardly accessible for humans. The area of civil application is very wide, and the examples are as follows: pipelines and power lines inspection and surveillance, oil and natural gas search, fire prevention, topography, agricultural applications, entertainment, etc.

Within the last years, rapid development of small and powerful microcontrollers, access to cheap and relatively accurate inertial sensors, reliable wireless links and finally efficient control systems allowed to advance some formerly existing aerodynamic configurations that were very difficult to control by human pilots only, like quadrotors. The most popular multirotor configuration is undoubtedly quadrotor [1], [3-8], [14]. This platform has been widely developed by many universities such as MIT or Stanford/Berkeley, and commercial companies like Draganflyer, X3D-BL or Xaircraft. It became widespread thanks to its mechanical simplicity and easily understandable dynamics - it is fully symmetrical. Its configuration includes even number of rotors aligned symmetrically and rotating pairwise in counter directions.

Many constraints such as weight, size and power consumption play an important role in unmanned systems efficiency, particularly in rotorcraft. The main goal of this work was to design and build a simple, light and durable airframe carrying embedded measurement and control system capable of autonomous hover, which minimizes energy consumption. The main intention was to decrease the number of motors to three. However the odd number of rotors and/or non-symmetrical alignment brings in uncompensated forces acting on the object. This makes the modeling and control of an unsymmetrical aircraft far more complex, since the excessive forces have to be explicitly compensated by the more advanced control system. For this reason, such constructions are not so popular although some interesting solutions can be found in the literature [2], [9], [10]. In the selection of multirotor configuration, the economic considerations can play a significant role that militate in favor of trirotor – smaller amount of rotors and ESC (Electronic Speed Control) modules.

During the whole work on the project three large research fields were investigated: UAVs mechanical design, navigation, stabilization and control algorithms. In this article we will focus on various aspects of control problems, ranging from the structure of the control system through the applied algorithms, ending at practical implementation of a full control of an under-actuated, inherently unstable system.

The paper is organized as follows. First, a mechanical design of the trirotor is introduced. The next part presents a hardware and measurement system, general structure of a cascade control system, and investigation of a PID controllers with modified loop structure. This section includes the detailed schemes and discussion of practical aspects of the control system implementation. The next section describes a rapid prototyping of designed embedded control system. Finally, the results of experiments are shown in chapter 5. The conclusions are briefly discussed in the last section.

A. Ryś, R. Czyba, and G. Szafrański are with the Silesian University of Technology, Akademicka 16, 44-100 Gliwice, Poland (corresponding author to provide phone: +48322371095; fax: +48322371165; e-mail: Roman.Czyba@polsl.pl).

978-1-4799-2376-2/14/$31.00 ©2014 IEEE

II. TRIROTOR - MECHANICAL DESIGN

A. *Flight dynamics*

A trirotor is an under-actuated system of 6 DOF and four actuators; three engines and one servomechanism. Two motors have fixed vertical position while the third one can be tilted by the servomechanism. Unlike a quadrotor, trirotor is not fully symmetrical object which introduces certain difficulties for the control system. Motion concept of a trirotor is shown in the Fig.1.

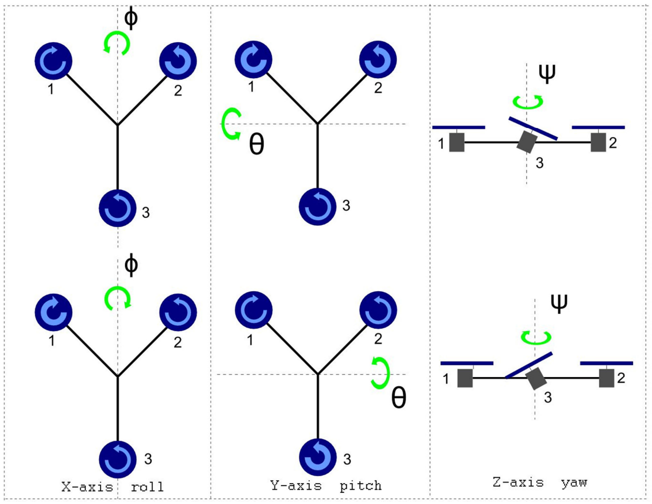

Figure 1. Trirotor motion concept.

If all rotors are spinning with the same angular velocity, the total torque causes rotation around yaw axis. Therefore, the engine 3 is tilted which decomposes the generated thrust into lift force and a component acting in opposite direction to the unbalanced torque. The tilt angle can be adjusted resulting in rotation around yaw axis. Roll angle changes are achieved by generating unbalanced forces by engines 1 and 2. Whereas changes of pitch angle are caused by unequal forces produced by engine 3 and sum of engines 1 and 2.

B. *Airframe*

Designing the airframe from scratch involved research in physics, aerodynamics, materials engineering, manufacturing and assembling techniques. The airframe should be possibly durable, stiff and light, therefore the materials chosen for the project were carbon fibre reinforced polymer (CFRP), aluminium, and polyamide PA 66. CFRP was used for side booms while the combination of aluminium and PA 66 were used for motors holders, tilt mechanism and central part. The airframe design in 3D CAD is shown in Fig.2, Fig.3, Fig.4.

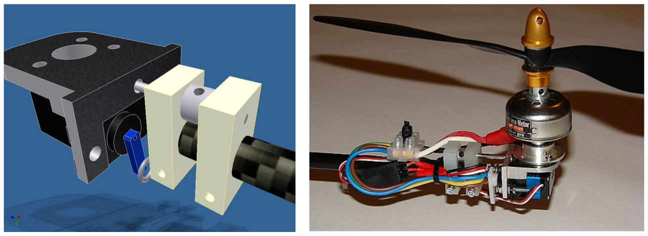

Figure 2. Tilt mechanism (design and assembly).

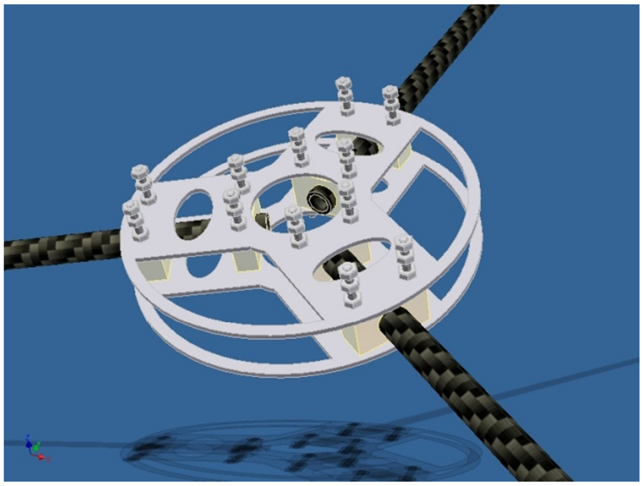

Figure 3. Central part assembly.

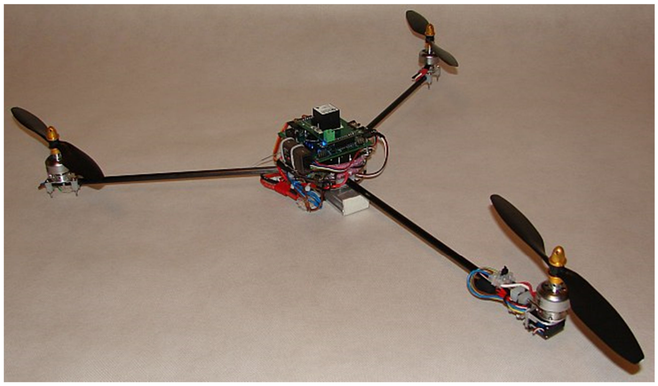

Figure 4. Assembled trirotor.

General specification for trirotor prototype is presented in Table I.

TABLE I. TECHNICAL SPECIFICATION

Parameter	Value (unit)
mass	750 (g)
top diameter	73 (cm)
payload	100 (g)
flight time	~ 15 (min)

III. CONTROL SYSTEM

A. *Hardware and Measurement System*

Autopilot plays a key role in each unmanned aerial system. The embedded electronics have been fully designed and manufactured in the framework of this project. The autopilot circuits are composed of two PCB boards. The main board performs data collection, solves navigation equations, reads and interprets orders from RC receiver, runs stabilization algorithms and controls the motors and servo. The second board is a measurement system which is based on the Analog Devices ADIS16400. It is an integrated device containing triaxial MEMS gyroscope, accelerometer, magnetometer and auxiliary analogue – digital converter.

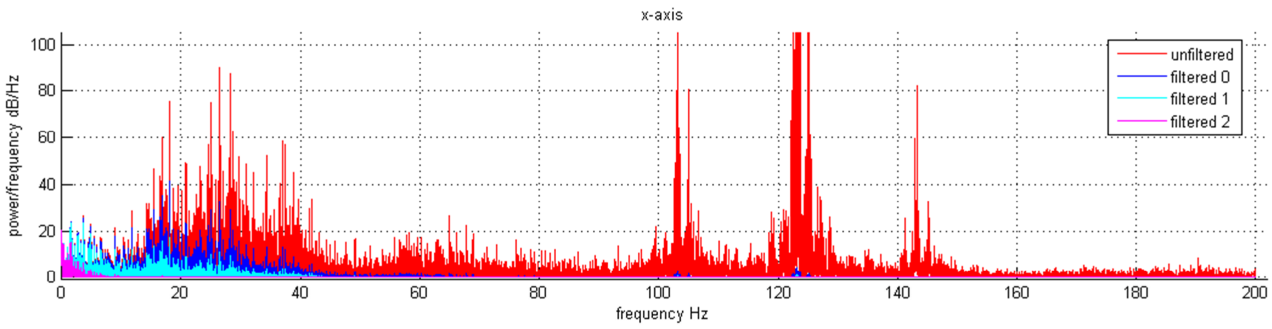

Figure 5. Periodogram of filtered and unfiltered gyro measurements

Due to the MEMS sensors nature, a noise in output signal is unavoidable. Additionally, running motors generate vibrations of wide spectrum. Digital linear, time-invariant (LTI) filters can be defined by a difference equation of the following form:

$$y[n] = \sum_{j=0}^{N} b_i x[n-j] - \sum_{i=1}^{M} a_i y[n-i] \qquad (1)$$

where: a_i – feedback coefficients, b_j – feed forward coefficients.

The following graph (Fig.5) shows the PSD (Power Spectral Density) estimate of unfiltered and filtered gyroscope measurements taken in vibrating environment.

TABLE II. FILTERS PARAMETERS

	FILTER 0 $\omega_c = 20Hz$		FILTER 1 $\omega_c = 10Hz$		FILTER 2 $\omega_c = 5Hz$	
	a	b	a	b	a	b
1	1.0000	0.1367	1.0000	0.0730	1.0000	0.0155
2	-0.7265	0.1367	0.0730	0.0730	-0.9691	0.0155

The analysis of the measurements frequency spectrum has shown two ranges mostly influenced by noise. The high frequency noise in the area ranging from 80 to 160Hz could have been easily filtered out without any negative effect on the navigation system. However, the low frequency noise appearing between 20 and 40Hz was more difficult to cope with. Applying a low-pass filter with cut-off frequency lower than 20Hz and strong attenuation in the stop band caused a significant increase of navigation response time, especially on rapid rotations. The issue has been solved by designing IIR Butterworth filter with cut-off frequency in range 10-20Hz and with wide transition band. The exemplary filters coefficients are presented in Table II.

During the research on INS (Inertial Navigation System), an efficient, Magdwick algorithm for MARG (Magnetic, Angular Rate and Gravity) sensor was found [11]. It is an interesting approach due to a very low computational load, quaternions internal implementation and high accuracy comparable with KF (Kalman Filter) solutions. After some modifications that increased robustness and performance, it has been integrated into trirotor's Attitude and Heading Reference System (AHRS).

B. General System Structure

The objective of the control algorithm for trirotor was stabilization of angles, in other words, ability to track and maintain given roll, pitch and yaw angles. The control system was decoupled and as a result each of the axes has a separate control algorithm. Three control algorithms return separate inputs for three engines and servomechanism which are combined with throttle signal in a mixer. The general system structure is presented in the Fig.6.

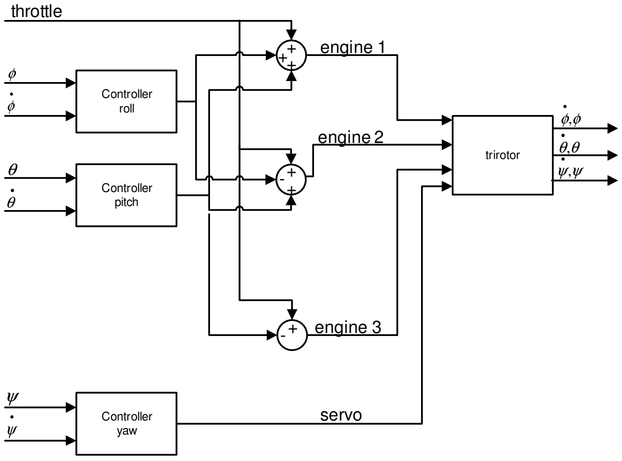

Figure 6. General system structure

System state is estimated according to the measurements obtained from a MARG sensors array. As it was already shown, ADIS16400 provides information about current angular velocity, linear acceleration and magnetic field orientation, with sample rate up to 819,2Hz. The raw readings are processed by a navigation algorithm which outputs the information about current UAV orientation. It is important to note, that the raw measurements, especially angular velocities, are of much faster dynamics than the attitude orientation returned by navigation algorithm. The reason is that they are measured directly by sensors, while the navigation algorithm introduces some extra dynamics.

C. Cascade Control System

According to the research on existing control systems for UAVs and investigation of measured characteristics a cascade structure was chosen for realization of trirotor control algorithm. An example of the control system of one control channel is presented in the Fig.7. Basically, in a cascade control schema the plant has one input and two or more outputs [12]. Indeed, this requires an additional sensor to be employed so that the fast dynamics could be measured. The primary controller and the primary dynamics are components of the outer loop. The inner loop is also a part of the outer loop, since the primary controller calculates the set point for the secondary controller loop. Furthermore the inner loop represents the fast dynamics, whereas the outer should be significantly slower (with respect to the inner loop). This assumption allows interaction that can occur between the loops to be restrained, improving stability. Therefore a higher gain in the inner loop can be adopted. An additional advantage is that the plant nonlinearities are handled by the controller in the inner loop, and exert no meaningful influence on the outer loop.

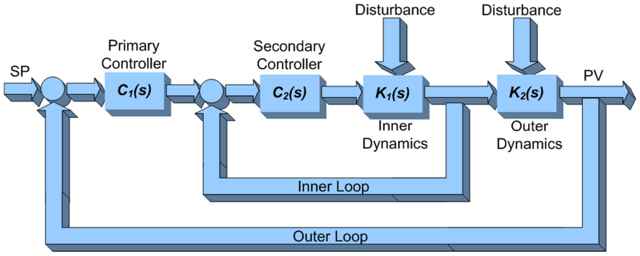

Figure 7. Cascade control system

In this paper the cascade control structure is proposed, as a solution to a control task formulated as an angular stabilization. Angular velocities of the rotating platform are used in the inner loop, whereas the outer loop is based on the Euler angles.

D. Control Algorithm

Nowadays, a number of different controllers are used in UAV applications. Those controllers can be divided into two main categories: classical, such as P, PI, PD, PID, and unconventional controllers. From the viewpoint of control theory, the UAV platform such as trirotor is highly nonlinear, nonstationary and multivariable plant. However, such a platform can be controlled by PID controllers in a satisfactory manner. Practical experience shows that this kind of control can be truly valuable, mostly due to its simplicity and straightforward design. It can be used to solve even a very complex control problems, especially when combined with diverse functional blocks, filters (compensators or correction blocks), selectors etc. There are multiple variations of the PID controller structure. In various sources, the controllers are named with different conventions, which sometimes is very confusing, especially when the same names are used for dissimilar structures, classified according to different criteria [12], [13].

The detailed structure of the control system of roll angle is shown in Fig.8. System structures for pitch and yaw control have the same structure.

The structure of controller chosen for the internal loop is of type B with filtered derivative [12]. The type B structure was selected in order to avoid undesired overreactions on changes in setpoint. Moreover, a filter in the derivative term provides additional control quality improvement. This loop guarantees quick reaction on disturbances in the system and easies tuning of the inherently unstable system. The outer loop, similarly to the inner one, is of type B with filtered derivative, however, there are some modifications introduced. The first modification concerns the way the setpoint changes are applied to the system. The main concern behind it is to reduce the overshoot when the setpoint varies rapidly. One method to avoid this problem would be to use type C PID controller. Although it removes the overshoot, it might be too slow for aerial vehicle, because the desired value is being tracked only by the integral term. The method that was implemented in the trirotor algorithm is a low-pass filter which reduces the speed of change of the setpoint to 10deg/s which is slow enough to avoid peak reaction of proportional term, and on the other hand, fast enough to provide high UAV performance.

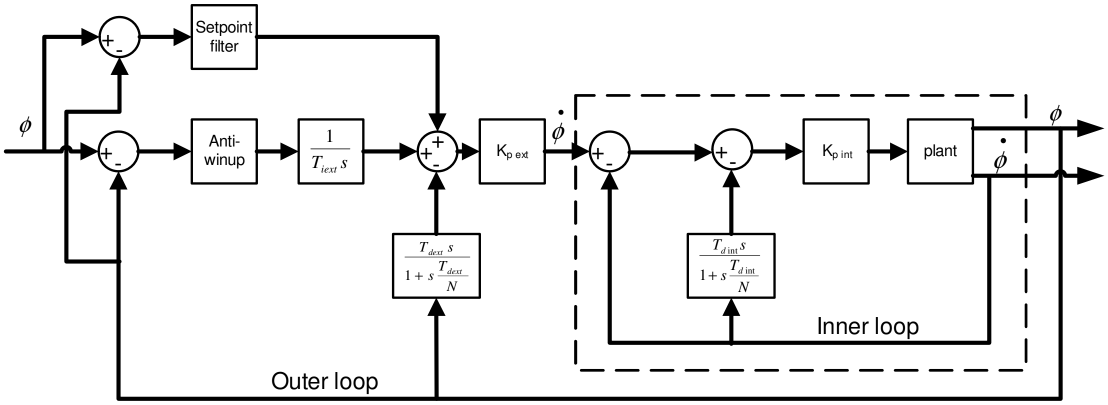

Figure 8. Detailed structure of trirotor controller

The second algorithm enhancement is a double anti-windup protection system. It limits the maximal value of error that supplies the integral part and defines lower and upper bound for the integral term value. The third enhancement of the algorithm is a filter in derivative term.

In the next sections the above control aspects will be discussed.

E. PID controllers with modified loop structure

The other problem with classical PID controllers is their reaction to a step change in the reference input which produces an impulse function in the controller action. There are two sources of the violent controller reaction, the proportional term and derivative term. Therefore, there are two PID controller structures that can avoid this issue. In literature exists different names [12], [17]: type B and type C; derivative-of-output controller and set-point-on-I-only controller; PI-D and I-PD controllers. The general idea of the modified designs is to move either the derivative term or both derivative and proportional term from the main path to the feedback path. Therefore, they are not directly vulnerable to set point discontinuities, while their influence on the control reaction is preserved, since the change in set point will be still transferred by the remaining terms. The structures of type B (PI-D) and type C (I-PD) are shown in Fig.9, Fig.10.

1) Type B PID controller

It is more suitable in practical implementation to use "derivative of output controller form". The equation of type B controller is following:

$$u(t) = K_p \left[e(t) + \frac{1}{T_i} \int_0^t e(\tau) d\tau - T_d \frac{dy(t)}{dt} \right] \qquad (1)$$

where: K_p – proportional gain, T_i – integral time constant, T_d– derivative time constant.

A block diagram that illustrates given controller structure is shown in Fig. 9. If PI-D structure is used, discontinuity in r(t) will be still transferred through proportional into control signal, but it will not have so strong effect as if it was amplified by derivative element.

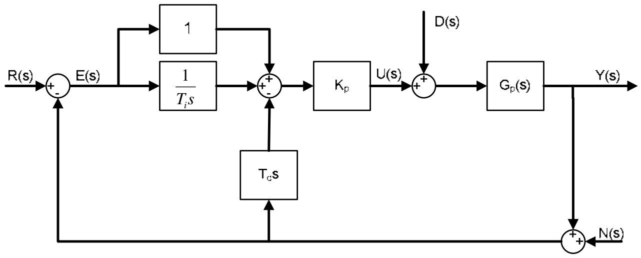

Figure 9. Type B PID controller

2) Type C PID controller

This structure is not so often used as PI-D structure, but it has certain advantages. Control law for this structure is given as:

$$u(t) = K_p \left[-y(t) + \frac{1}{T_i} \int_0^t e(\tau) d\tau - T_d \frac{dy(t)}{dt} \right] \qquad (2)$$

Block diagram for type C controller is shown in Fig.10.

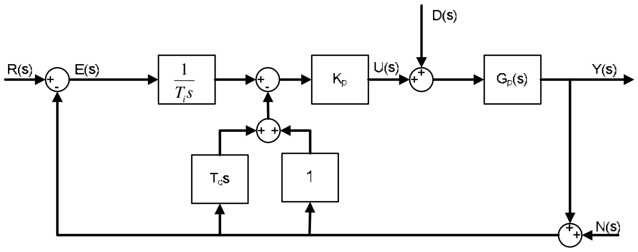

Figure 10. Type C PID controller

With this structure transfer of reference value discontinuities to control signal is completely avoided. Control signal has smoother changes than with other structures.

F. PID controller with filtered derivative

The ideal PID controller has an improper transfer function structure. Thus, its practical implementation is impossible. The main reason is the derivative term that causes large distortion in the control signal when high-frequency noise is present in the control loop. This problem can be significantly reduced by an additional filter in the derivative term. A common filter used to decrease the gain at higher frequencies is a first order inertia (Fig.11).

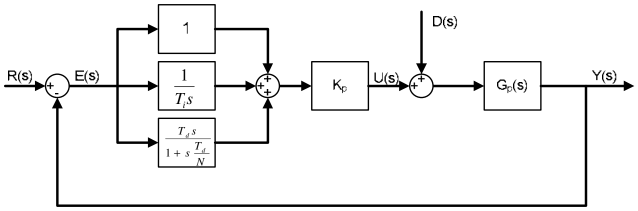

Figure 11. PID controller with filtered derivative

The approximation can be regarded as an ideal derivative sT_d filtered by a first order inertia with the time constant $\frac{T_d}{N}$. Thus, the approximation works as a derivative for low-frequency signal components with the gain limited to N.

This solution is suitable for all other PID controllers with modified loop structure.

G. Integral windup

All real actuators have certain natural physical limitations e.g.: a motor speed, a tilt angle of servomechanism, etc. When an actuator reaches its physical limitation, a controller saturation occurs. In this case, the integral term will accumulate large error, the larger, the longer the saturation lasts. This situation happens usually when a large setpoint change is applied to the system. As a result, there might appear long periods of overshoot in the controlled response which slow down the controller reaction.

This negative feature is called integral windup and should be eliminated from practical implementations of PID controllers. In this work to accomplish this task two following methods was applied.

1) Setpoint limitation

The first method introduce constraints on the setpoint changes, so that the controller never exceeds the physical limitations of actuator. The constraints on setpoint changes can limit the maximal change in setpoint by defining a valid range of changes or they can modify the setpoint changes to form of a suitable ramp/time profile. More sophisticated research on this issue can be found in [15].

2) Back calculation

Discussed technique is presented in the Fig.12.

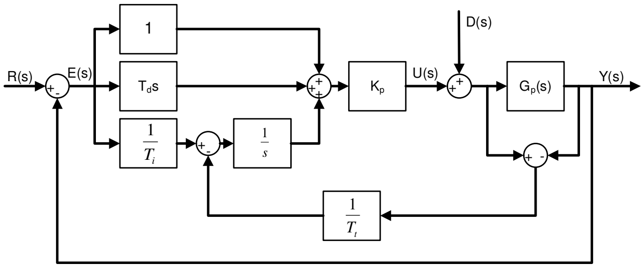

Figure 12. PID controller with back calculation anti-windup method

This method is based on comparing of the controller output with the actual actuator value. When these values are equal then the difference of them is zero and there is no influence on the algorithm. However, when the controller output falls outside the usable actuator input range, it means that the saturation occurred and the further increasing (decreasing for lower bound) of the algorithm output is undesirable. Therefore, the calculated difference is multiplied by a gain and fed back to the integral term. As a result, the integral term is supplied with lowered value or, if the gain is large enough, with a value of opposite sign, which improves an estimate of the correct state of the controller when it is not matching the real actuator input values.

IV. RAPID PROTOTYPING OF EMBEDDED CONTROL SYSTEM

The system configuration used for tests and tuning purposes is presented in the Fig.13. This structure was used for a fast prototyping of designed attitude control system in the hardware in the loop structure (HiL).

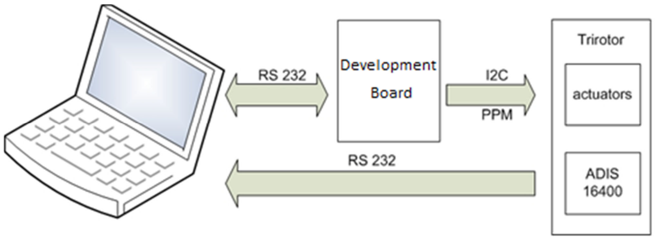

Figure 13. System configuration for control system rapid prototyping

In order to enable the interaction between unmanned platform and the operator, it is necessary to provide dedicated interface and adequate Ground Control Station (GCS) Software. The application has a user-friendly graphical interface (GUI) that provides real-time visualization of all operations which are being performed. Application's main window is shown in the Fig.14, Fig.15.

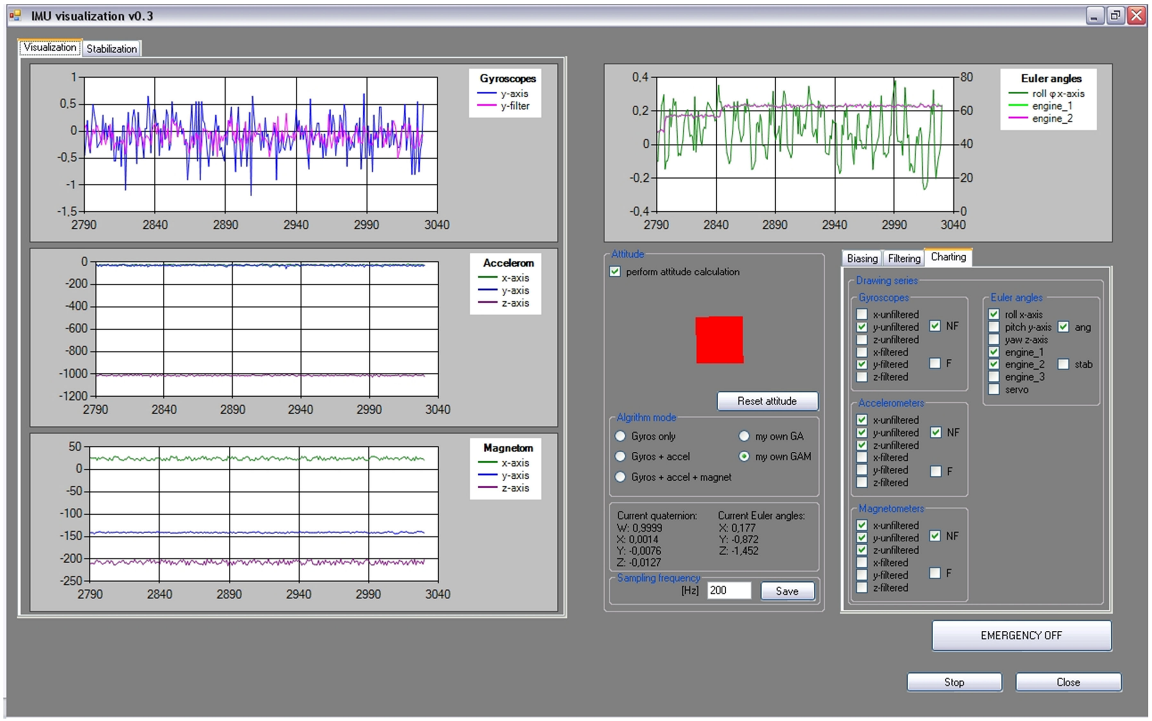

Attitude

☑ perform attitude calculation

Algrithm mode

○ Gyros only ○ my own GA

○ Gyros + accel ● my own GAM

○ Gyros + accel + magnet

Current quaternion:
W: 0,9999
X: 0,0014
Y: -0,0076
Z: -0,0127

Current Euler angles:
X: 0,177
Y: -0,872
Z: -1,452

Sampling frequency [Hz] 200

Drawing series

Gyroscopes
☐ x-unfiltered
☑ y-unfiltered ☑ NF
☐ z-unfiltered
☐ x-filtered
☑ y-filtered ☐ F
☐ z-filtered

Accelerometers
☑ x-unfiltered
☑ y-unfiltered ☑ NF
☑ z-unfiltered
☐ x-filtered
☐ y-filtered ☐ F
☐ z-filtered

Magnetometers
☑ x-unfiltered
☑ y-unfiltered ☑ NF
☑ z-unfiltered
☐ x-filtered
☐ y-filtered ☐ F
☐ z-filtered

Euler angles
☑ roll x-axis
☐ pitch y-axis ☑ ang
☐ yaw z-axis
☑ engine_1
☑ engine_2 ☐ stab
☐ engine_3
☐ servo

Figure 14. GCS application main window – visualuzation tab

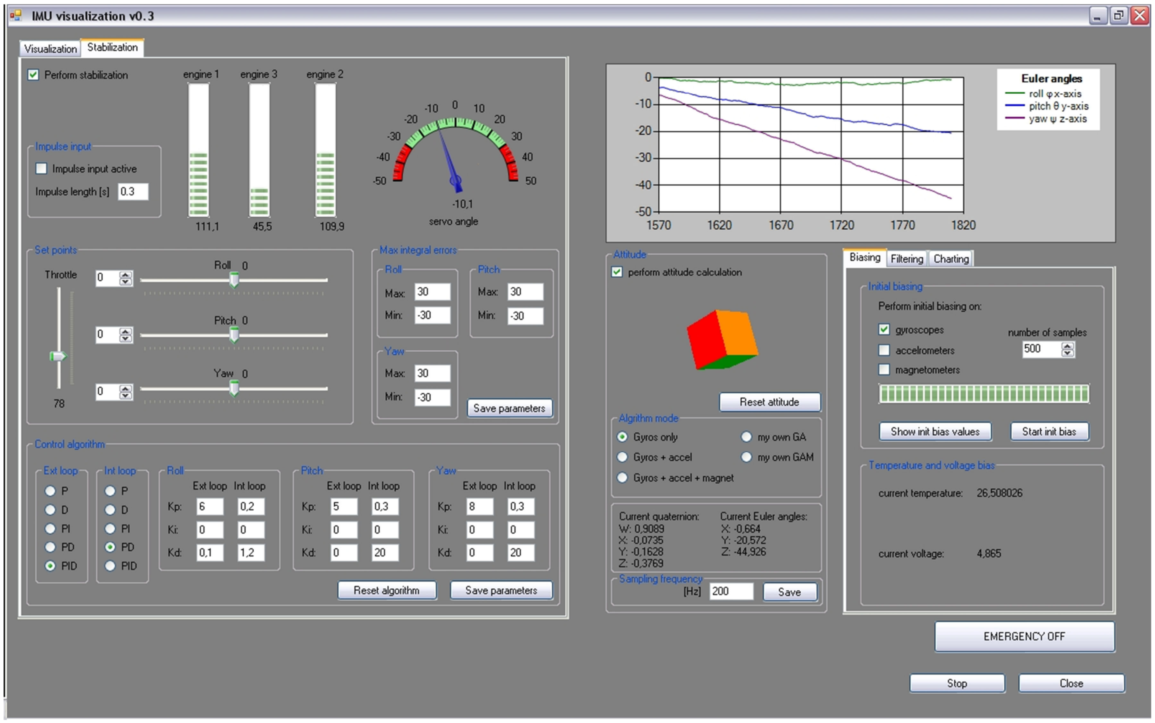

☑ Perform stabilization

☐ Impulse input active

Impulse length [s] 0.3

Throttle 0, 78

Roll 0: 0

Pitch 0: 0

Yaw 0: 0

	Roll	Pitch	Yaw
Max:	30	30	30
Min:	-30	-30	-30

Ext loop: ○ P ○ D ○ PI ○ PD ● PID

Int loop: ○ P ○ D ○ PI ● PD ○ PID

	Roll Ext loop	Roll Int loop	Pitch Ext loop	Pitch Int loop	Yaw Ext loop	Yaw Int loop
Kp:	6	0,2	5	0,3	8	0,3
Ki:	0	0	0	0	0	0
Kd:	0,1	1,2	0	20	0	20

☑ perform attitude calculation

Algrithm mode: ● Gyros only ○ Gyros + accel ○ Gyros + accel + magnet ○ my own GA ○ my own GAM

Current quaternion:
W: 0,9089
X: -0,0735
Y: -0,1628
Z: -0,3769

Current Euler angles:
X: -0,664
Y: -20,572
Z: -44,926

Sampling frequency [Hz] 200 Save

Perform initial biasing on:
☑ gyroscopes
☐ accelrometers
☐ magnetometers

number of samples 500

current temperature: 26,508026

current voltage: 4,865

Figure 15. GCS application main window – stabilization and control tab

The three charts on the left side display real-time data collected from ADIS16400. The charts can display either raw or filtered and biased measurements or both simultaneously. The displayed series can be modified during run time in the tab Charting. The tab Biasing allows to start initial bias procedure with a given samples number and displays the current temperature and voltage readings returned by ADIS16400. The tab Filtering allows to input arbitrary FIR or IIR digital filter. The order of filter can be specified along with its coefficients. The filter coefficients input form is compatible with Matlab filter designing tools. Maximum three different filters can be defined, all filtering independently chosen sensors. The chart displays angles values and the cubicle represents the actual rotation of MARG sensor array in three dimensions. The current value of quaternion and Euler angles calculated by navigation algorithm are also presented in the group box. The currently used navigation algorithm version can be selected in run time.

The tab Stabilization is used to modify the settings relevant to the control algorithms, define setpoints as well as visualize the algorithms operation. It allows also to change the control loop settings like controller type and tune the controller parameters in the HiL configuration in real time while algorithms are operating.

Another test stand was used to tune up the three axes simultaneously. The stand provided a free fly possibility with 6DOF, however, for the safety reasons it limited UAV displacements.

V. TEST RESULTS

In this section, we present the results of experiment which was conducted on the constructed tilt trirotor, to evaluate the performance of the designed control system. The tests were performed in order to examine whether all components are working properly and stabilization of trirotor attitude is possible. The ability to maintain a given setpoint for at least 60 seconds was tested for each axis separately using a specialized stand that limited the number of degrees of freedom to one. The tuning process followed cascade systems tuning rules i.e. the inner loop was tuned to have possibly high proportional and derivative gain. These setting provided good rejection of disturbances appearing in the inner loop. Secondly, the outer loop having slower dynamics was tuned so, that the trirotor was able to maintain a given setpoint. Tests results were satisfactory, the trirotor was able to hold a given setpoint for unlimited time. After several tests performed on the experimental setup, it was time to test an autonomous flight. Once the trirotor was capable of maintaining a given constant setpoint, tests against step changes were performed. The gains required slight modifications in order to prevent a overshoot to occur and provide damping of oscillations. The tests have proven that the trirotor is properly tracking changes in setpoints in all axes. The results are presented in Fig.16.

VI. CONCLUSION

In this paper, a single tilt trirotor unmanned platform is presented, beginning with the mechanical design, through the hardware, till the measurement and control system architecture with particular emphasis on the practical aspects of the control implementation.

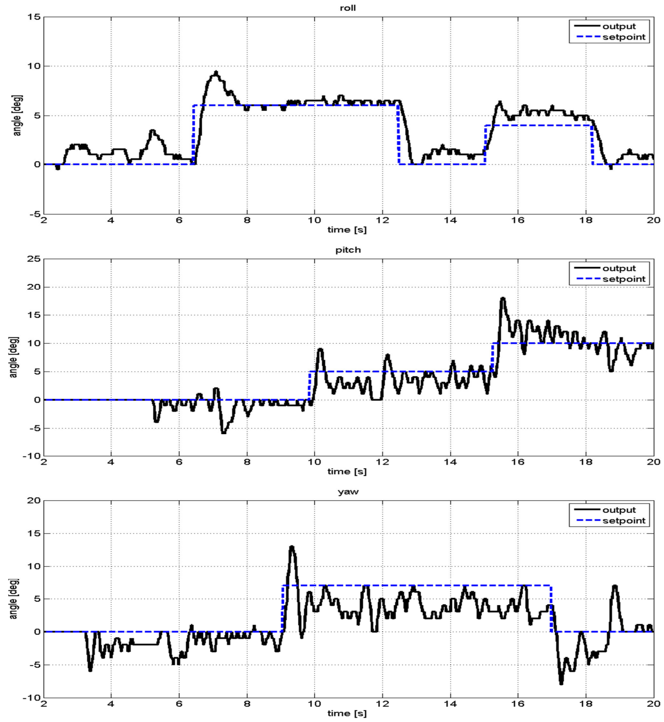

Figure 16. Tracking of the Euler angles setpoints

A research of this UAV configuration required building a platform from scratch because, in opposite to quadrotor, there are not many commercially available trirotors. In this work much attention was paid to an overview of control approaches used for UAVs control. Various PID controllers structures suitable for practical implementations have been shown. The setpoint kick in proportional and derivative terms, integral windup, and accurate approximation of derivative action have been discussed. Additionally, a cascade PID control system has been introduced together with the requirements and constraints for the system to validate cascade control system application. According to the results of the research on practical control systems, an appropriate system for the trirotor was developed in the form of a cascade PID and PD positional controllers of type B with filtered derivative terms, double integral windup protection and limited setpoint changes ratio. The next section contains a description of the application that has been developed in an effort to have an convenient, high-performance and user-friendly working environment. The system configuration allows for fast prototyping of designed attitude control system, and in particular for tests and tuning the controller parameters. Finally, the trirotor performance tests results including tracking changes in setpoint for all axes has been presented. The obtained results confirm that tilting mechanism greatly increase the maneuverability in yawing axis of the VTOL platform. In the future research, on the basis of comparison between tri- and quad-rotor it will be possible to assess the capability of minimizing energy consumption in developed construction.

ACKNOWLEDGMENT

This work has been granted by the Polish Ministry of Science and Higher Education from funds for years 2014-2015.

The author Grzegorz Szafrański is a scholar from the "DoktoRIS - Scholarship Program for Silesian Innovation" co-funded by the European Union from the European Social Fund.

REFERENCES

[1] A. Tayebi and S. McGilvray, *Attitude stabilization of a VTOL quadrotor aircraft*, IEEE Trans. on Control Systems Technology, vol. 14, no. 3, 2006, pp. 562-571.

[2] J.S. Chiou, H.K. Tran and S.T. Peng, *Attitude Control of a Single Tilt Tri-Rotor UAV System: Dynamic Modeling and Each Channel's Nonlinear Controllers Design.* Mathematical Problems in Engineering, vol. 2013, Hindawi Publishing Corporation, 2013.

[3] K. Nonami, F. Kendoul, S. Suzuki, W. Wang, Nakzawa D., *Autonomous Flying Robots*. London: Spirnger, 1st edition, 2010.

[4] I.A. Raptis, K.P. Valavanis, *Linear and Nonlinear Control of Small-scale Unmanned Helicopters*. Dordrecht: Springer-Verlag, 2011.

[5] K.P. Valavanis, *Advances in Unmanned Aerial Vehicles.* The Netherlands: Springer-Verlag, 2007.

[6] P. Castillo, R. Lozano, and A. E. Dzul, *Modelling and Control of Mini-flying Machines.* London: Springer-Verlag, 2005, ch. 3.

[7] M.D. Hua, T. Hamel, P. Morin, C. Samson, *Introduction to Feedback Control of Underactuated VTOL Vehicles.* IEEE Control Systems Magazine, February 2013, pp. 61-75.

[8] P.J. Bristeau, F. Callou, D. Vissiere, *The Navigation and Control technology inside the AR.Drone micro UAV*. Preprints of the 18th IFAC World Congress, Milano, 2011, pp.1477-1484.

[9] S. Salazar, R. Lozano, J. Escareño,.. *Stabilization and nonlinear control for a novel trirotor mini-aircraft*. Proceedings of the 2005 IEEE International Conference on Robotics and Automation, Barcelona, Spain, pp. 2612-2617.

[10] J. Escareño, A. Sanchez, O. Garcia, R. Lozano, *Triple Tilting Rotor mini-UAV: Modeling and Embedded Control of the Attitude*, American Control Conference, Westin Seattle Hotel, Seattle, Washington, USA, June 11-13, 2008.

[11] S.O.H. Magdwick, A.J.L. Harrison, R. Vaidyanathan, *Estimation of IMU and MARG orientation using a gradient descent algorithm*. IEEE International Conference on Rehabilitation Robotics, Switzerland, June 29 – July 1, 2011.

[12] A. Visioli, *Practical PID control*, Springer 2006.

[13] K.H. Ang, G. Chong, Y. Li, *PID Control System Analysis, Design, and Technology*. July, 2005, IEEE Transaction on Control Systems Technology, vol. 13 no.4.

[14] R. Zawiski, M. Błachuta, *Chosen aspects of modelling and control of quadrotor platform.* AIP Conference Proceedings 1493 of 9th International Conference on Mathematical Problems in Engineering, Aerospace and Sciences: ICNPAA 2012, pp. 1116-1123, 10-14 July, Vienna.

[15] V. D. Yurkevich, *Design of Nonlinear Control Systems with the Highest Derivative in Feedback.* World Scientific Publishing, 2004.

[16] http://www.tealgroup.com

[17] H. L. Wade, *Basic and Advanced Regulatory Control: System Design and application.* ISA, United States of America, 2004.